



# CD22-targeted CAR T cells induce remission in B-ALL that is naive or resistant to CD19-targeted CAR immunotherapy

Terry J Fry<sup>1</sup> , Nirali N Shah<sup>1</sup>, Rimas J Orentas<sup>1,8</sup>, Maryalice Stetler-Stevenson<sup>2</sup>, Constance M Yuan<sup>2</sup>, Sneha Ramakrishna<sup>1</sup>, Pamela Wolters<sup>1</sup>, Staci Martin<sup>1</sup>, Cindy Delbrook<sup>1</sup>, Bonnie Yates<sup>1</sup>, Haneen Shalabi<sup>1</sup>, Thomas J Fountaine<sup>1</sup>, Jack F Shern<sup>1</sup>, Robbie G Majzner<sup>3</sup>, David F Stroncek<sup>4</sup>, Marianna Sabatino<sup>4</sup>, Yang Feng<sup>5</sup>, Dimiter S Dimitrov<sup>5</sup>, Ling Zhang<sup>1</sup>, Sang Nguyen<sup>1</sup>, Haiying Qin<sup>1</sup>, Boro Dropulic<sup>6,8</sup>, Daniel W Lee<sup>1,8</sup> & Crystal L Mackall<sup>7</sup> 

Chimeric antigen receptor (CAR) T cells targeting CD19 mediate potent effects in relapsed and/or refractory pre-B cell acute lymphoblastic leukemia (B-ALL), but antigen loss is a frequent cause of resistance to CD19-targeted immunotherapy. CD22 is also expressed in most cases of B-ALL and is usually retained following CD19 loss. We report results from a phase 1 trial testing a new CD22-targeted CAR (CD22-CAR) in 21 children and adults, including 17 who were previously treated with CD19-directed immunotherapy. Dose-dependent antileukemic activity was observed, with complete remission obtained in 73% (11/15) of patients receiving  $\geq 1 \times 10^6$  CD22-CAR T cells per kg body weight, including 5 of 5 patients with CD19<sup>dim</sup> or CD19<sup>-</sup> B-ALL. Median remission duration was 6 months. Relapses were associated with diminished CD22 site density that likely permitted CD22<sup>+</sup> cell escape from killing by CD22-CAR T cells. These results are the first to establish the clinical activity of a CD22-CAR in B-ALL, including leukemia resistant to anti-CD19 immunotherapy, demonstrating potency against B-ALL comparable to that of CD19-CAR at biologically active doses. Our results also highlight the critical role played by antigen density in regulating CAR function.

Cure rates for children with B-ALL approach 90%, but outcomes for those with relapsed and chemotherapy-refractory disease remain poor<sup>1,2</sup>. Adults with B-ALL experience survival rates of <50% even when treated with pediatric therapy-inspired, risk-adapted, multi-agent regimens<sup>3–5</sup>. Risk-adapted therapy can diminish the prevalence of severe late effects in survivors, but long-term morbidity remains substantial, especially in patients treated with intensive regimens for high-risk disease<sup>6,7</sup>.

Immunotherapies targeting CD19 have recently provided a new class of effective therapeutics for B-ALL. Blinatumomab, a CD19–CD3-bispecific antibody, mediates impressive effects in patients with overt<sup>8,9</sup> and minimal residual disease (MRD) levels of B-ALL<sup>10</sup>. T cells expressing CARs targeting CD19 have also demonstrated impressive antileukemic effects in children and adults with relapsed and/or refractory B-ALL, with remission rates ranging from 70–90% (refs. 11–13). However, the likelihood of durable remission following CD19-targeted immunotherapy remains unknown. Although CD19 is expressed by essentially all cases of B-ALL at clinical presentation<sup>14,15</sup>, relapses with loss or diminished cell-surface expression of CD19 are increasingly recognized as a cause of treatment failure<sup>12,16–18</sup>.

Like CD19, CD22 is expressed by most cases of pre-B-ALL<sup>14,19,20</sup>, and normal tissue expression is restricted to the B cell lineage. Substantial clinical experience and success has been reported with monoclonal antibody-based therapeutics targeting CD22 (refs. 21–29). We report the first clinical experience, to our knowledge, using a CD22-CAR as therapy for B-ALL<sup>19,30</sup>. Our data demonstrate that CD22-CAR T cells have a similar safety profile to that of CD19-CAR T cells and mediate similarly potent anti-leukemic effects in both immunotherapy-naïve patients and patients with CD19<sup>dim</sup> or CD19<sup>-</sup> relapse following CD19-directed immunotherapy. These results are the first to establish that CAR T cells targeting antigens other than CD19 can mediate similarly potent antineoplastic effects and to demonstrate that resistance to immunotherapy via antigen loss can be overcome by treatment with CAR T cells targeting an alternative antigen, opening the way for dual-targeted immunotherapeutics.

## RESULTS

### Patient characteristics

The first 21 consecutive patients with relapsed or refractory B-ALL treated with CD22-CAR T cells are included in this analysis.

<sup>1</sup>Pediatric Oncology Branch, Center for Cancer Research, National Institutes of Health (NIH), Bethesda, Maryland, USA. <sup>2</sup>Laboratory of Pathology, Center for Cancer Research, NIH, Bethesda, Maryland, USA. <sup>3</sup>Department of Pediatrics, Stanford University, Stanford, California, USA. <sup>4</sup>Department of Transfusion Medicine, NIH Clinical Center, NIH, Bethesda, Maryland, USA. <sup>5</sup>Cancer and Inflammation Program, National Cancer Institute, NIH, Bethesda, Maryland, USA. <sup>6</sup>Lentigen Corporation, Gaithersburg, Maryland, USA. <sup>7</sup>Department of Pediatrics and Stanford Cancer Center, Stanford University, Stanford, California, USA. <sup>8</sup>Present addresses: Lentigen Technology, Inc., Miltenyi Biotec, Gaithersburg, Maryland, USA (B.D. and R.J.O.) and Division of Pediatric Hematology & Oncology, Department of Pediatrics, University of Virginia, Charlottesville, Virginia, USA (D.W.L.). Correspondence should be addressed to T.J. Fry ([fryt@mail.nih.gov](mailto:fryt@mail.nih.gov)).

Received 8 February; accepted 13 October; published online 20 November 2017; doi:10.1038/nm.4441

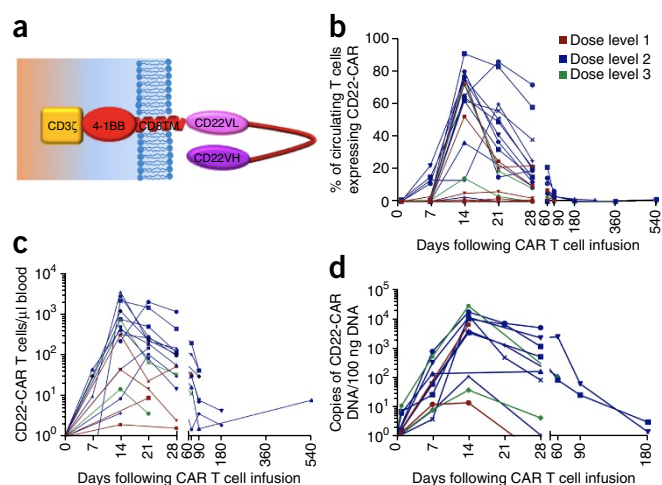


**Figure 1** Expansion of the CD22-CAR T cells infused following lymphodepleting chemotherapy. (a) Schematic of the CD22-CAR. CD3 $\zeta$ , CD3 zeta domain; CD8 TM, CD8 transmembrane domain; CD22VL, anti-CD22 variable light chain; CD22VH, anti-CD22 variable heavy chain. (b) Percentage of circulating T cells that express the CD22-CAR, as measured through flow cytometry. (c) Absolute number of circulating CD22-CAR T cells per microliter blood calculated by multiplying the percentage of CD22-CAR $^{+}$  T cells by the absolute number of CD3 $^{+}$  T cells per microliter blood. (d) The number of copies of the integrated CD22-CAR transgene per 100 ng DNA obtained from peripheral blood mononuclear cells.

The median age was 19 years (range, 7–30 years); all patients had undergone at least one prior hematopoietic stem cell transplantation (HSCT), and two patients had each received two prior HSCTs (Supplementary Table 1). Seventeen patients had received prior CD19-directed immunotherapy, including 15 who received CD19-targeted CAR (CD19-CAR) therapy. Lymphoblasts were CD19 $^{-}$  or CD19 $^{dim}$  in ten patients, including nine following CD19-CAR therapy and one following treatment with blinatumomab. Median bone marrow blast percentage was 70.5% (range, 1–99%), and all were classified as central nervous system 1 (CNS1; <5 white blood cells (WBC)/ $\mu$ l blood and no blasts). Median CD22 site density was 2,839 molecules per cell (range, 613–13,452). Fourteen patients exhibited B cell aplasia at the time of enrollment (B cell counts, <50 cells/ $\mu$ l blood), including seven patients who had received prior therapy with a CD19-CAR, suggesting that the patients experienced ongoing effects from the previous CAR therapy. All treated patients received the intended protocol-specified dose of T cells modified to express the anti-CD22 CAR construct, which was based on a previously reported binding domain<sup>30</sup> that was modified to incorporate a 4-1BB endodomain, which has been shown to improve persistence<sup>31</sup>. A schematic of the anti-CD22 CAR construct is shown in Figure 1a. Characteristics of the infused products containing CD22-CAR T cells are shown in Supplementary Table 2.

### Toxicity

The primary toxicity experienced by patients was cytokine release syndrome (CRS)<sup>11–13</sup>, which occurred in 16 of 21 patients, coincided with CAR T cell expansion and began after day 5 of treatment in all patients in whom it developed. Protocol-defined (Online Methods) grade 1 CRS occurred in nine patients, and grade 2 CRS occurred in seven patients. Patient 2 experienced grade 3 self-limited, noninfectious diarrhea during CRS, which resolved with supportive care; however, it resulted in dose-limiting toxicity (DLT) at the first dose level, requiring a protocol-specified expansion of the first

dose level to six patients. No further DLTs were observed at the first dose level. Three patients subsequently received dose level 2 ( $1 \times 10^6$  CD22-CAR T cells per kg body weight) with no evidence of DLT. Two patients then proceeded to dose level 3 ( $3 \times 10^6$  CD22-CAR T cells per kg body weight), and patient 10 developed dose-limiting grade 4 hypoxia that was associated with rapid disease progression. The patient required brief intubation, and complete resolution of the hypoxia occurred within 24 h of initiation of steroid treatment. A second patient was safely treated at this dose level without DLT. On the basis of the single case of DLT at dose level 3 and the clinical activity associated with substantial CD22-CAR T cell expansion and persistence at dose level 2, a dose of  $1 \times 10^6$  CD22-CAR T cells per kg body weight was identified as the recommended phase 2 dose, and the cohort was expanded to include ten additional patients ( $n = 13$  total at dose level 2). One subject (patient 14) with a pre-enrollment history of multiorgan failure due to sepsis died from gram-negative rod sepsis that developed after resolution of CRS and neutrophil count recovery to >1,000 cells/ $\mu$ l blood. Prospective neurotoxicity evaluations demonstrated no irreversible neurotoxicity or seizure. Among the first 16 patients with complete assessments, transient visual hallucinations ( $n = 2$ ), mild unresponsiveness ( $n = 1$ ), mild disorientation ( $n = 1$ ) and mild-moderate pain ( $n = 2$ ) were observed but returned to baseline by day 28 post-infusion. B cell aplasia (<50 cells/ $\mu$ l blood) was noted in all patients who achieved remission, including patients who were not previously B cell aplastic. Grade 3–4 toxicities possibly, probably or definitely attributed to the CD22-CAR are listed in Supplementary Table 3.

### CD22-CAR T cells demonstrate robust expansion and antileukemic activity

Data regarding CAR T cell expansion, persistence and response for individual patients are summarized in Supplementary Table 4. CD22-CAR T cells were detected in the peripheral blood in 19 of 21 treated patients and peaked on day 14 (Fig. 1). The median peak expansion was 62% of circulating T cells expressing the CD22-CAR (Fig. 1b; range 1–91%), the median number of circulating CAR T cells was 316 cells/ $\mu$ l blood (Fig. 1c; range, 1–3,593 cells/ $\mu$ l blood) and the median peak expansion in the first 16 patients, as measured through PCR of the CAR DNA sequence, was 7,007 copies/100 ng DNA (Fig. 1d; range, 15–30,500 copies/100 ng DNA). On day 28, CAR T cells remained detectable in the peripheral blood in 15 of 21 patients, in the bone marrow in 15 of 19 patients for whom bone marrow flow cytometry was performed (median, 25%; range, 0–78.2%) and in the cerebrospinal fluid (CSF) in 12 of 17 patients for whom CSF analysis was performed (range, 21–71.6%). CAR T cells remained detectable in the blood of seven of nine patients evaluated 3 months post-infusion, in two of three patients evaluated at 6 months post-infusion, and in one patient evaluated at 9 months post-infusion and one patient evaluated at 18 months post-infusion, both of whom were in ongoing remission at the time points at which they were evaluated.

Twelve patients (57%) achieved complete remission (CR) (Figure 2a); nine were MRD negative (Supplementary Table 4). Response varied with the administered cell dose. At the first dose level ( $3 \times 10^5$  CD22-CAR T cells per kg body weight), 1 of 6 patients attained CR as compared to 11 of 15 patients (73%) at doses of  $\geq 1 \times 10^6$  CD22-CAR T cells per kg body weight ( $P < 0.001$ , Fisher's exact test). Among patients receiving  $\geq 1 \times 10^6$  CD22-CAR T cells per kg body weight, CR occurred in nine of ten patients who had received prior CD19-directed immunotherapy, including all five patients who enrolled with

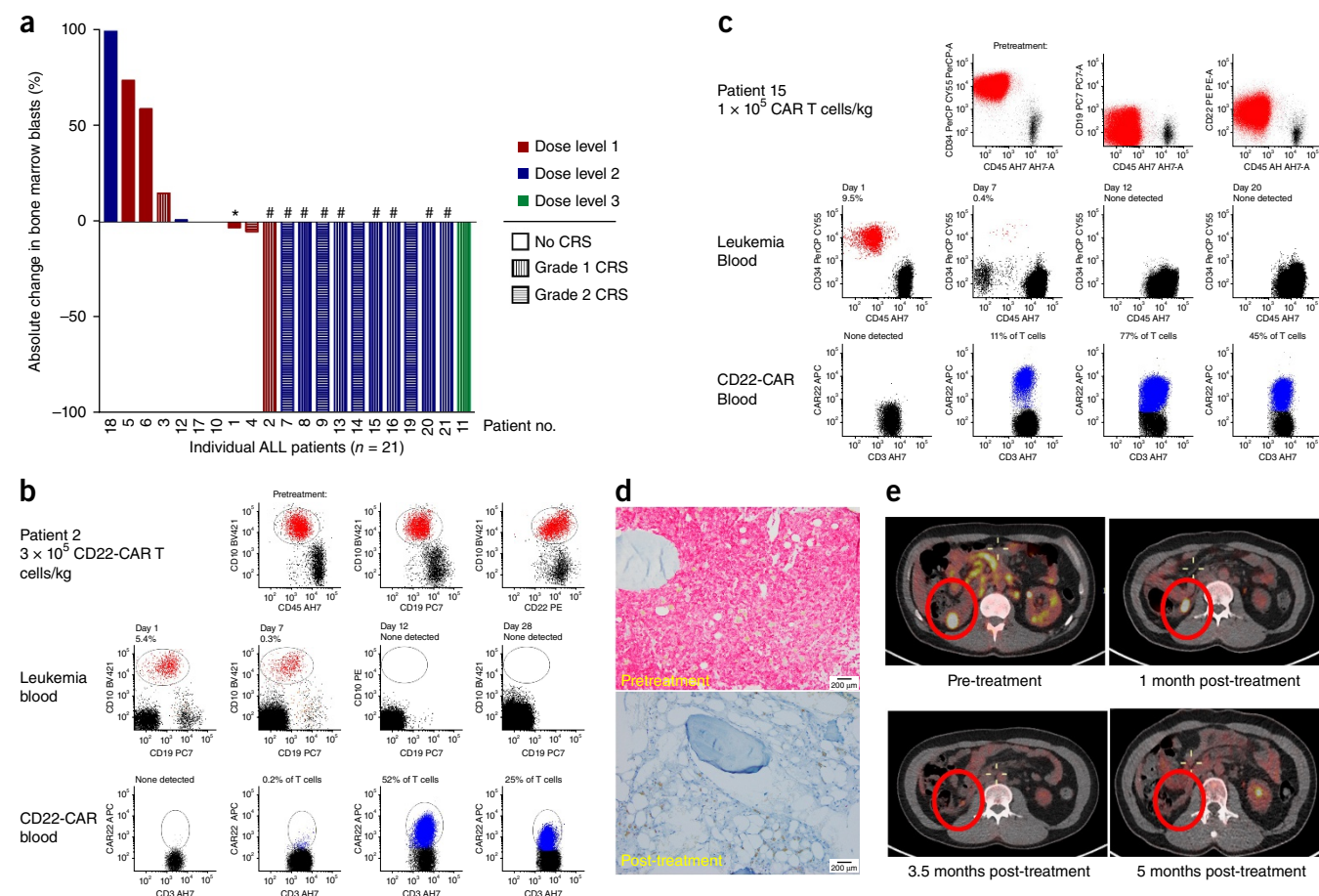


**Figure 2** CD22-CAR T cells induce remission in patients with relapsed and refractory pre-B-ALL, including ALL resistant to CD19-CAR T cells. (a) Waterfall plot showing the percentage change in bone marrow aspirate blast frequency from baseline to day 28 ( $\pm 4$  d) and CRS grading in the first 21 consecutive patients treated. \*, a patient with progressive disease (PD) defined as greater than a 50% increase in circulating blasts; #, a patient who achieved MRD-negative CR. (b) Eradication of CD19<sup>dim</sup> ALL relapsing after CD19-CAR T cell therapy following infusion of  $3 \times 10^5$  CD22-CAR T cells/kg body weight (cells/kg) in patient 2. Top row, cell-surface antigen expression of leukemia cells in bone marrow. Bottom two rows, clearance of circulating blasts (upper) and CAR T cell expansion (lower) in blood. (c) CAR T cell expansion and clearance of CD19<sup>dim</sup> ALL resistant to CD19-CAR T cells following infusion of  $1 \times 10^6$  CD22-CAR T cells/kg body weight in patient 15. (d) Immunohistochemistry analysis of a bone marrow biopsy (staining for CD79A, a pan-B cell marker, in red) from patient 15, revealing MRD-negative CR and B cell aplasia at 1 month following CD22-CAR T cell infusion. Magnification, 200x. (e) Serial positron emission tomography (PET) scans showing pretreatment disease and evolution to full resolution in post-treatment evaluations in patient 13.

CD19<sup>dim</sup> or CD19<sup>-</sup> B-ALL and one patient who was refractory to both CD19-CAR and blinatumomab therapies (patient 11). Thus, we saw no evidence that previous CD19-directed immunotherapy or diminished surface expression of CD19 impacted response to CD22-CAR T cells. **Figure 2b** illustrates response in patient 2, whose leukemia exhibited diminished CD19 surface expression and who had substantial disease burden; this patient experienced MRD-negative CR following infusion of  $3 \times 10^5$  CAR T cells per kg body weight. Similarly, patient 15 had complete absence of cell-surface CD19 expression and high disease burden, but attained MRD-negative remission with grade 1 CRS and considerable lymphocyte expansion (**Fig. 2c,d**). Responses were also seen in patients with extramedullary disease, including patient 13, who attained MRD-negative bone marrow remission at day 28 with a steady decrease in fluorodeoxyglucose uptake in lymphomatous disease, which fully resolved by 5 months following CAR infusion (**Fig. 2e**).

Among the four nonresponders at dose levels 2 and 3, two (patients 10 and 18) had very high disease burden with rapid disease progression, which may have contributed to their lack of response. Two

additional nonresponders (patients 12 and 17) expressed diminished or partial CD22 on leukemic blasts at the time of enrollment; this emerged following administration of inotuzumab ozogamicin, an anti-CD22-calicheamicin conjugate<sup>29</sup>, immediately before enrollment on this study.

Serum cytokines were measured serially in all patients during the first month following therapy initiation (**Supplementary Figs. 1 and 2**, images from representative patients). Similar to previous reports following CD19-CAR T cell therapy, we saw a general correlation between high leukemia burden and high peak cytokine levels, as illustrated by patient 4 and patient 9.

#### Relapse is associated with diminished CD22 site density without detectable CD22 mutations or changes in CD22 mRNA levels

Among the 12 patients who attained CR, 3 remained in ongoing CR at 21 months, 9 months and 6 months (**Supplementary Table 4**). Eight patients relapsed at 1.5–12 months (median, 6 months) following CD22-CAR infusion, and relapse was associated with diminished



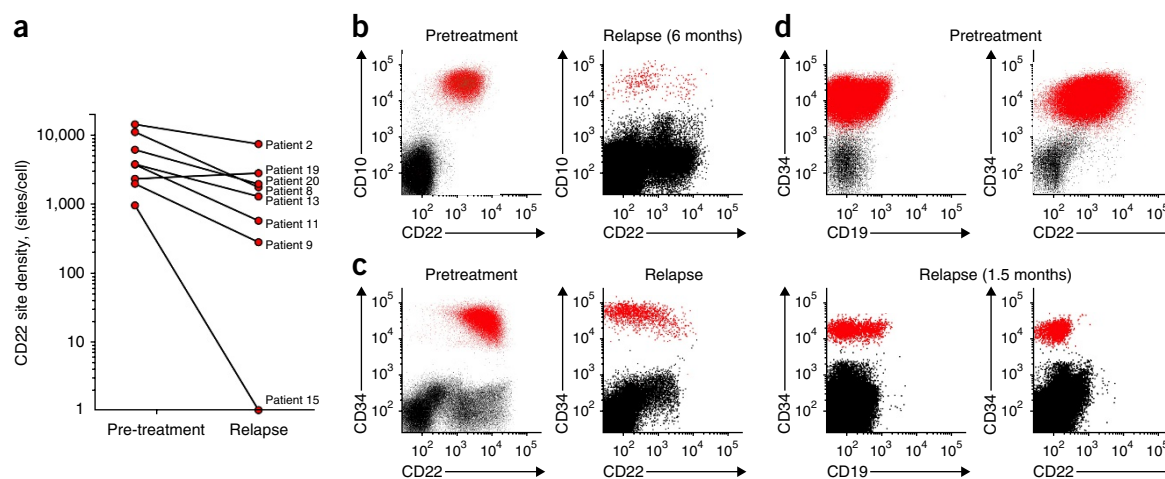


**Figure 3** Changes in CD22 cell-surface expression in a subset of patients following CD22-CAR T cell infusion. **(a)** Change in CD22 cell-surface expression in patients achieving remission following CD22-CAR T cell therapy who subsequently developed relapse. **(b)** Patient 9, who enrolled with CD19<sup>+</sup> B-ALL, experienced MRD-negative remission following CD22-CAR T cell therapy with subsequent relapse at 6 months, demonstrating the emergence of two leukemic cell populations with altered CD22 expression as compared to the pretreatment condition. **(c)** Relapse with CD22<sup>+</sup> ALL following MRD-negative remission in patient 15 who had CD19<sup>+</sup> ALL prior to treatment. The last therapy for this patient before CD22-CAR T cells was inotuzumab ozogamicin. At the time of relapse, 23% of the T cells in the bone marrow and 14.4% of the T cells in the peripheral blood were CD22-CAR<sup>+</sup>. **(d)** Patient 11 relapsed with CD22<sup>+</sup> B-ALL at 1.5 months following CD22-CAR T cell infusion. The therapy administered immediately before CD22-CAR T cells was inotuzumab ozogamicin.

CD22 surface expression in seven patients (Fig. 3a). An illustrative example is provided by patient 9, who enrolled with CD19<sup>+</sup> leukemia and experienced relapse at 6 months following CD22-CAR therapy with blasts that were both CD19<sup>+</sup> and CD22<sup>+</sup> (Fig. 3b). Two patients who enrolled after receiving inotuzumab ozogamicin experienced early relapse, including patient 11, who relapsed at 1.5 months following CD22-CAR T cell infusion with low but variable CD22 surface expression on leukemic blasts (Fig. 3c), and patient 15, who had CD19<sup>+</sup> leukemia following CD19-CAR therapy and relapsed with variable CD22 surface expression that was diminished to negative at 2 months following CD22-CAR T cell infusion (Fig. 3d) despite high levels of circulating CD22-CAR T cells (Fig. 2c).

Rather than the persistent and complete absence of target that has been reported following CD19-directed immunotherapy due to preferential expression of CD19 splice variants in resistant leukemia lacking the targeted epitope<sup>16</sup>, we observed a pattern of acquired resistance to the CD22-CAR associated with diminished (Fig. 3) and variable (Supplementary Fig. 3) CD22 site density, as assessed by flow cytometry (Online Methods). To determine whether diminished CD22 site density may have had a causal role in relapse in this setting through enabling escape of low-CD22-site-density (CD22<sup>lo</sup>) leukemic blasts from CD22-CAR T cells, we assessed the functionality of the CD22-CAR against NALM6-derived cell lines engineered to express varying CD22 site densities reflecting the range that was observed in this study (Fig. 4a). Interferon (IFN)- $\gamma$  (Fig. 4b) and IL-2 (Fig. 4c) production by CD22-CAR T cells was reduced following exposure to NALM6 cells expressing a low CD22 density corresponding to levels observed at the time of relapse in patients following CD22-CAR therapy. Finally, although CD22-CAR T cells delay *in vivo* progression of CD22<sup>lo</sup> ALL, leukemia progression eventually ensues (Fig. 4d). These results implicate diminished CD22 surface expression on B-ALL cells as a mechanism for relapse following CD22-CAR therapy.

To identify possible genetic or transcriptomic mechanisms underlying the observed alteration in CD22 site density, longitudinal assessment of the CD22 genomic locus and corresponding mRNA

was undertaken in two patients with diminished CD22 site density who relapsed following CD22-CAR treatment. Genome-wide copy number profiles of their leukemias remained stable despite substantial changes in CD22 site density. Heterozygosity at the CD22 locus was maintained, and no focal copy number changes were observed. Mutation analysis comparing the pretreatment and post-treatment samples demonstrated no acquired mutations within the CD22 locus (Fig. 5a and Supplementary Fig. 4a). Corresponding analysis of CD22 mRNA levels before and after CD22-CAR treatment revealed no qualitative change in the observed CD22 transcripts and provided no evidence for diminished transcription of CD22, as in each case total CD22 mRNA levels were slightly increased at the time that CD22 site density was diminished (Fig. 5b and Supplementary Fig. 4b). We saw no evidence for alternative CD22 isoforms as a cause of the observed downmodulation of CD22, although a new isoform cannot be ruled out. Furthermore, we studied a patient-derived xenograft model (PDX) in mice subjected to immune pressure with CD22-CAR T cells, which induced complete loss of CD22 cell-surface expression. Remarkably, such leukemias again showed no evidence of genetic mutation, changes in gene copy number or isoform expression, or diminished mRNA expression (Fig. 5c–e). Together, the data implicate post-transcriptional effects in modulating CD22 protein levels rather than genomic mutation, modulation of gene expression or altered isoform expression.

#### A bispecific CAR targeting both CD19 and CD22 can recognize and kill CD19<sup>+</sup>CD22<sup>+</sup>, CD19<sup>+</sup>CD22<sup>+</sup> and CD19<sup>+</sup>CD22<sup>+</sup> B-ALL

Multiagent combination chemotherapy is a central tenet of ALL therapy. The results presented here establish robust clinical activity of a new CAR-based therapeutic for the treatment of B-ALL, but they also illustrate the challenges associated with sequential administration of CD19-CAR followed by CD22-CAR therapy. We therefore sought to develop a bispecific CAR T cell that could simultaneously recognize CD19- and CD22-expressing targets. Using a single CAR construct that incorporates both CD19 and CD22 single-chain variable

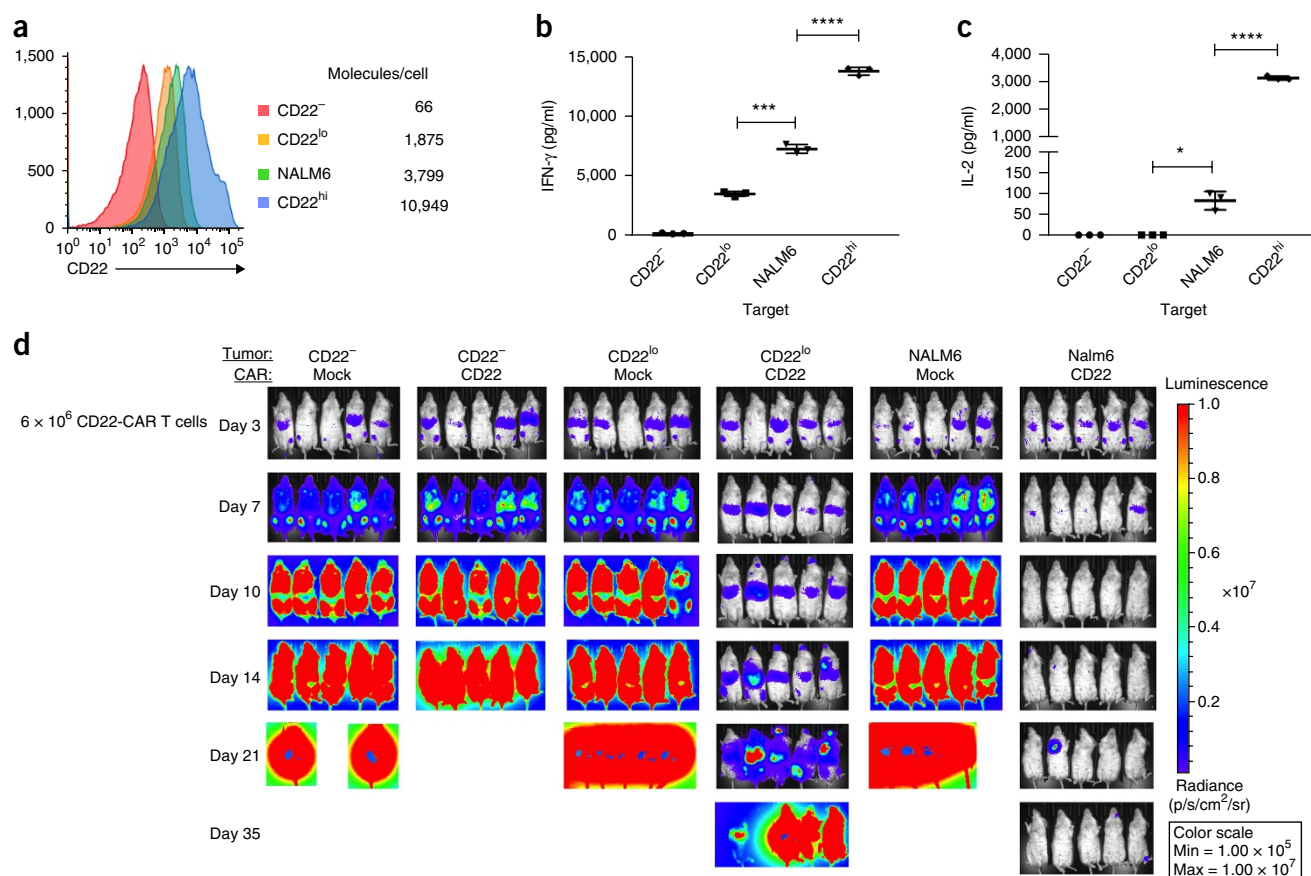


**Figure 4** CD22 site density limits CD22-CAR functionality. **(a)** Histogram of CD22 expression on CRISPR–Cas9-edited NALM6-derived CD22<sup>low</sup> B-ALL lines transduced to express varying levels of CD22. The table lists site density using the same flow cytometry–based assay that was used to measure CD22 expression by patient samples. **(b,c)** IFN-γ **(b)** and IL-2 **(c)** production by CD22-CAR-transduced T cells upon co-culture with NALM6 cell lines with varying CD22 site densities. \**P* < 0.05, \*\*\**P* < 0.005, \*\*\*\**P* < 0.001 by one-way ANOVA. Data shown in **b** and **c** are representative of three independent experiments. Lines represent means ± s.e.m. from triplicate wells. **(d)** PDX model demonstrating clearance of parental NALM6 cells by CD22-CAR T cells at a dose of  $6 \times 10^6$  CAR T cells per mouse administered at day 3 following B-ALL cell injection but failure of the same CAR T cells to eradicate NALM6 cells with low CD22 site density despite initial delay in leukemia progression. Bioluminescence serves as a proxy for disease burden in NALM6 leukemia cells engineered to express luciferase after treatment with luciferin. The data are representative of three independent experiments.

fragment (scFv) sequences into one bivalent receptor (**Fig. 6a**), we demonstrate *in vitro* cytokine production against and killing of CD19<sup>+</sup>CD22<sup>+</sup>, CD19<sup>+</sup>CD22<sup>low</sup> and CD19<sup>+</sup>CD22<sup>hi</sup> B-ALL cell lines (**Fig. 6b,c** and **Supplementary Fig. 5**). T cells transduced with this bispecific construct administered intravenously at a dose of  $3 \times 10^6$  cells per mouse into NOD-SCID gamma (NSG) mice 3 d after injection of luciferase-expressing B-ALL demonstrated the ability to clear B-ALL (**Fig. 6d**). Thus, the binding domain in the CD22-CAR validated in the clinical trial reported here can be combined with a CD19-binding domain validated as a CAR construct in multiple clinical trials to generate a single multitargeted CAR construct with the potential to overcome the leukemic resistance arising when either CAR is administered alone.

## DISCUSSION

CD22, a sialic acid-binding immunoglobulin-like lectin (SIGLEC) expressed exclusively within the B cell lineage, is expressed on the vast majority of B cell malignancies, including B-ALL, indolent and high-grade non-Hodgkin's lymphoma, chronic lymphocytic leukemia and hairy cell leukemia<sup>14,19,20,32,33</sup>. Numerous CD22-directed therapeutics have been studied in clinical trials. Epratuzumab, an unconjugated anti-CD22 monoclonal antibody, mediated modest clinical

activity in adult and pediatric B-ALL<sup>21,26,27</sup>. CD22 immunotoxins mediated clinical activity in hairy cell leukemia<sup>23</sup> and B-ALL<sup>22</sup>, but benefits were transient owing to the short half-life of the agent and substantial immunogenicity. A recent phase 3 trial of inotuzumab ozogamicin, an anti-CD22 monoclonal antibody conjugated to the toxin calicheamicin, demonstrated complete responses in 80.7% of patients with relapsed and/or refractory B-ALL<sup>29</sup>. However, liver toxicity limited the dose intensity that could be safely delivered, and the agent is associated with higher rates of veno-occlusive disease following subsequent HSCT<sup>24,34</sup>.

We generated a new CAR targeting CD22, which we optimized by comparing potency across multiple scFvs and multiple co-stimulatory domains<sup>19,30,35</sup>. Therapeutics incorporating the scFv derived from the monoclonal antibody m971 binding domain<sup>30</sup> have not been tested previously in clinical trials. The data presented here demonstrate potent antileukemic activity with modest CRS and no evidence for off-target toxicity following CD22-CAR therapy. Doses of  $\geq 1 \times 10^6$  CD22-CAR T cells per kg body weight mediated substantial antileukemic activity that was comparable to results obtained with CD19-CAR treatment, with 11 of 15 patients obtaining CR, including 8 of 10 patients previously treated with CD19-based immunotherapies and 5 of 5 patients who enrolled with CD19<sup>low</sup> or

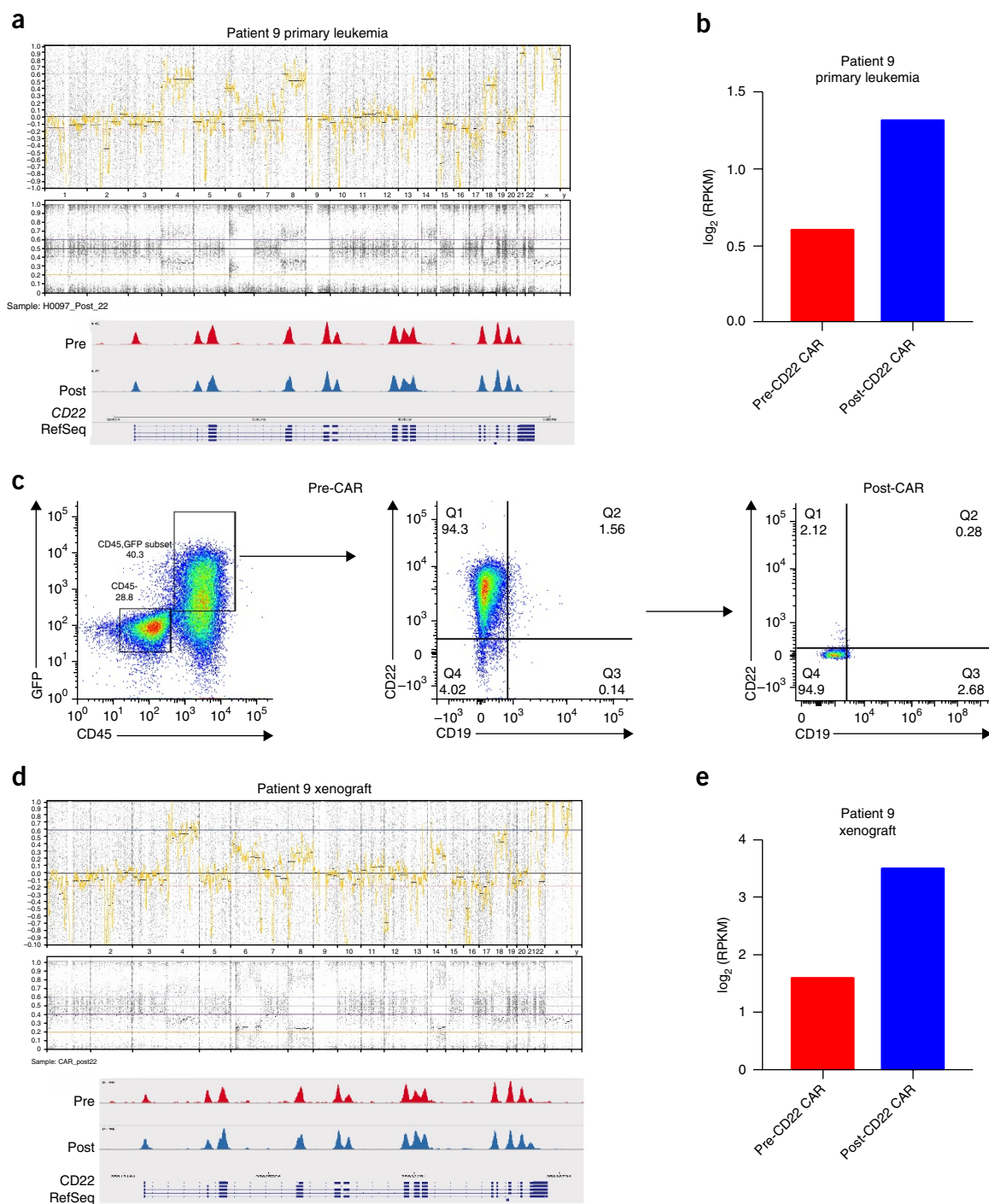


**Figure 5** Whole-exome and RNA-seq profiling of *CD22* in primary patient samples and a PDX model that recurred in the presence of CD22-CAR immunotherapeutic immune pressure. **(a)** Genome-wide copy number profiling of the primary and relapsed leukemia samples from patient 9 demonstrates no net ploidy changes across the genome. Interrogation of the *CD22* locus demonstrated no exon-level alteration in the pre- or post-treatment sample. **(b)** Analysis of RNA-seq data for patient 9 showed maintenance of *CD22* mRNA expression pre- and post-treatment. RPKM, reads per kilobase of transcript per million mapped reads. **(c)** A PDX model developed from patient 9 was treated *in vivo* with CD22-CAR T cells and showed tumor response; this was followed by relapse of leukemia without surface CD22 expression as determined through flow cytometry. **(d)** Genome-wide copy number and *CD22* exon analysis demonstrated genomic stability from the primary tumor with no copy number gains or losses and maintenance of the ploidy status before and after therapy. **(e)** *CD22* transcript levels in the pre- and post-treatment samples again showed maintenance of consistent mRNA expression.

CD19<sup>dim</sup> relapse. Notably, all enrolled patients had undergone previous HSCT, and patient 7, who had undergone two previous HSCTs before receiving the CD22-CAR T cells, has remained in remission 21 months following CD22-CAR therapy with persistent CAR T cells

and has received no additional antileukemic therapy since treatment with the CD22-CAR T cells. Together, the data provide no evidence to suggest that previous chemotherapy or CD19-based immunotherapy diminishes the likelihood of remission induction following



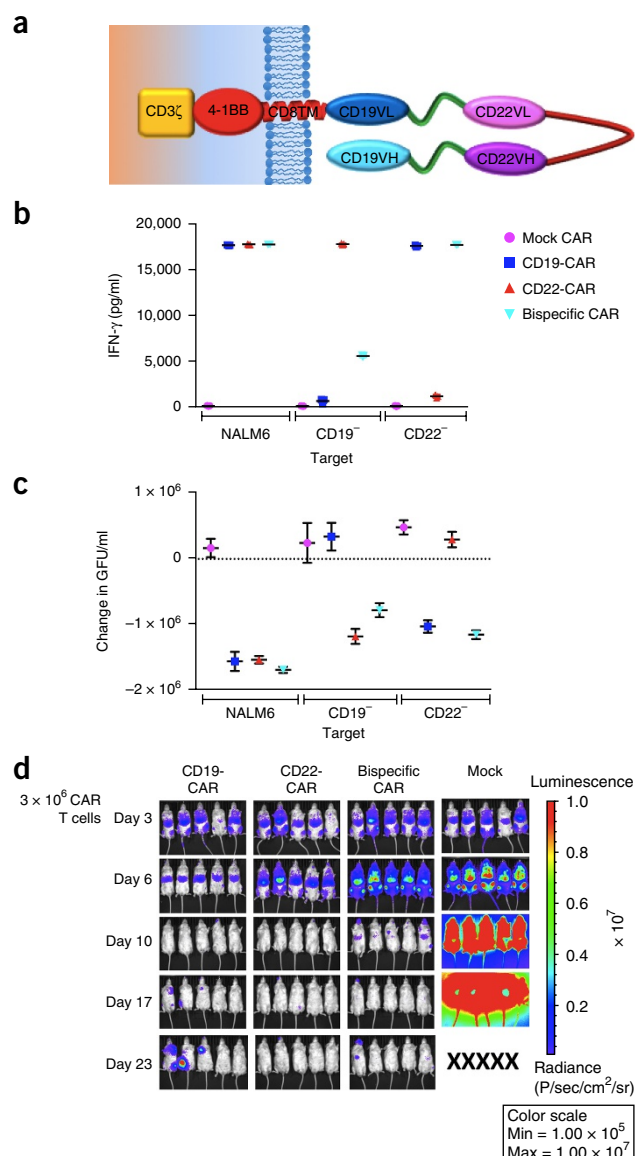


**Figure 6** The CD22-CD19-bispecific CAR demonstrates *in vitro* and *in vivo* activity against CD19-CD22<sup>+</sup> or CD19<sup>+</sup>CD22<sup>-</sup> ALL. **(a)** Schematic representation of the CD19-CD22-bispecific CAR construct. **(b,c)** IFN- $\gamma$  production in response to parental NALM6 and CRISPR-Cas9-edited CD19<sup>-</sup> and CD22<sup>-</sup> NALM6 cell lines as measured by enzyme-linked immunosorbent assay **(b)** and *in vitro* killing of CD19-CD22<sup>-</sup> NALM6 cell lines **(c)**. *In vitro* killing of GFP-expressing NALM6 ALL was measured by loss of GFP<sup>+</sup> cells. The data presented in **b** and **c** are representative of two independent experiments. GFU, green fluorescent units. Error bars represent standard error of measurement. **(d)** Eradication of NALM6-derived cells in mice by CAR T cells expressing the indicated constructs. The data are representative of four independent experiments.

administration of bioactive doses of CD22-CAR T cells. The CD22-CAR studied here incorporates a 4-1BB co-stimulatory endodomain, and the T cells expressing it demonstrate a pattern of expansion and persistence similar to that observed following therapy with CD19-CAR T cells incorporating a 4-1BB endodomain; this is consistent with previous evidence that the CAR co-stimulatory domains play a dominant role in modulating the rate of expansion and the likelihood of persistence following CAR therapy<sup>35</sup>. CD22-CAR T cells also migrated efficiently to the CSE, but we observed no evidence for

severe neurologic toxicity or seizures, which have been observed in studies of CD19-CAR therapy<sup>11–13</sup>.

CARs targeting CD19 have demonstrated remarkable activity in B-ALL and diffuse large B cell lymphoma (DLBCL), and we demonstrate similar complete response rates in B-ALL with the CD22-CAR tested here. This is notable because numerous non-CD19-targeted CARs have entered clinical trials for B cell malignancies (CD20-CAR<sup>36</sup>,  $\kappa$ -CAR<sup>37</sup>, CD138-CAR<sup>38</sup> and BCMA-CAR<sup>39</sup>), AML<sup>40</sup> and solid tumors, yet none of these have demonstrated complete response rates of >50%. This work therefore provides the first evidence that CD19 is not a uniquely effective target of CAR T cells and raises the prospect that similarly effective CARs could ultimately be developed for an array of antigenic targets. Future studies are needed to determine whether the high response rates observed with CD22-CARs in B-ALL will translate into similarly sizable response rates in DLBCL, in which CD22 expression is common.

CD19 is universally expressed at high levels on B-ALL at the time of diagnosis and is retained following cytotoxic therapy<sup>41–43</sup>. However, since the introduction of CD19-based immunotherapies, relapse with diminished or absent cell-surface CD19 has been increasingly observed and has emerged as the dominant mechanism of resistance to this class of therapeutics. CD19 immune escape was first reported following blinatumomab therapy<sup>10</sup> but has now been observed by several groups following CD19-CAR therapy<sup>12,44</sup>. In a recent report of 50 patients who entered remission with CD19-CAR therapy with a median follow-up of 10.6 months, 40% of patients had relapsed and loss of the CD19 target accounted for 65% of the total relapses<sup>17</sup>. Thus, although the true incidence is unknown, CD19 immune escape is emerging as the most common cause of relapse following CD19-CAR therapy for B-ALL. Recent investigation into the biology of ‘CD19-negative B-ALL’ has revealed that the majority of cases retain mRNA encoding CD19 but are enriched for CD19 isoforms that lack cell-surface expression or epitopes targeted by all CD19 immunotherapeutics currently under study<sup>16</sup>. An alternative pathway for loss of or diminished CD19 expression involves lineage switch of blasts with acquisition of myeloid markers and characteristics<sup>45</sup>. None of the patients enrolled on this study appeared to manifest CD19 loss associated with lineage switch.

The data presented here demonstrate that diminished CD22 site density, rather than total loss of surface expression, is sufficient to permit escape of leukemia from CD22-directed CAR therapy. This is not unique to the CD22-CAR but rather reflects a pattern observed across CARs, which demonstrate a requirement for increased target antigen levels relative to those required for activation of native T cell receptors<sup>46–49</sup>. Decrease in CD22 site density or complete CD22 loss was observed in seven of eight patients who relapsed following CD22-CAR-induced remission. Considering that CD22 surface expression is often variable at presentation, it appears likely that this phenomenon represents selection of pre-existing CD22<sup>lo</sup> cells within the heterogeneous leukemia population. Notably, we identified no genetic basis for the change in surface expression and no evidence for diminished mRNA levels in leukemic cells demonstrating low CD22 site density, thus implicating post-transcriptional mechanisms in this biology. Regardless of the mechanism, decades of experience with cytotoxic chemotherapy for B-ALL have convincingly established that multimodal chemotherapy is required to achieve long-term remission. We propose, on the basis of clear evidence for CD19 antigen loss or downregulation following CD19-directed immunotherapy and evidence for diminished CD22 cell-surface expression contributing to relapse following sequential CAR therapy,

that simultaneous immunotherapeutic targeting of multiple antigens may diminish the likelihood of tumor escape through antigen loss. Proof of principle for the bioactivity of a bispecific anti-CD19CD22-CAR in mice is demonstrated here.

In summary, the majority of patients who develop CD19 immune escape following CD19-directed immunotherapy retain CD22 surface expression, and this report demonstrates that such leukemias remain susceptible to immune-based targeting. Furthermore, although we demonstrate proof of principle for sequential immunotherapeutic targeting of a second antigen mediating clinical benefit, we also observe a high rate of relapse associated with diminished CD22 cell-surface expression using this approach, raising the prospect that simultaneous multispecific targeting may be a more effective approach to enhance the durability of immunotherapy-induced remission in B-ALL. Toward this end, we have developed a CAR that simultaneously targets both CD19 and CD22, which could prove more effective at inducing remissions and could be less susceptible to relapse associated with antigen escape<sup>50</sup>. Clinical trials testing this CD19–CD22-mutispecific CAR are underway.

## METHODS

Methods, including statements of data availability and any associated accession codes and references, are available in the [online version of the paper](#).

*Note: Any Supplementary Information and Source Data files are available in the online version of the paper.*

## ACKNOWLEDGMENTS

We gratefully acknowledge the study participants and their families, referring medical care teams, the faculty and staff of the NIH and the data managers involved with this work. This work was supported in part by the Intramural Research Program, National Cancer Institute and NIH Clinical Center, National Institutes of Health, by a Stand Up to Cancer–St. Baldrick's Pediatric Dream Team translational research grant (SU2C-AACR-DT113) and by a St. Baldrick's Foundation Scholar Award (D.W.L.). Stand Up to Cancer is a program of the Entertainment Industry Foundation administered by the American Association for Cancer Research. C.L.M. is a member of the Parker Institute for Cancer Immunotherapy, which supports the Stanford University Cancer Immunotherapy Program. The content of this publication does not necessarily reflect the views or policies of the Department of Health and Human Services, nor does mention of trade names, commercial products or organizations imply endorsement by the US government.

## AUTHOR CONTRIBUTIONS

T.J. Fry, N.N.S., R.J.O., D.S.D., B.D., D.W.L. and C.L.M. designed the study. T.J. Fry, N.N.S., M.S.-S., C.M.Y., C.D., B.Y., H.S., D.F.S., M.S., Y.F., P.W., S.M., D.W.L., T.J. Fountaine, J.E.S., L.Z., S.N., H.Q., P.W., S.R., R.G.M. and C.L.M. generated and analyzed the data. T.J. Fry, N.N.S. and C.L.M. vouch for the data and the analysis, wrote the paper and decided to publish the paper. No nonauthor wrote the first draft or any part of the paper.

## COMPETING FINANCIAL INTERESTS

The authors declare competing financial interests: details are available in the [online version of the paper](#).

Reprints and permissions information is available online at <http://www.nature.com/reprints/index.html>. Publisher's note: Springer Nature remains neutral with regard to jurisdictional claims in published maps and institutional affiliations.

- Smith, M.A., Altekruze, S.F., Adamson, P.C., Reaman, G.H. & Seibel, N.L. Declining childhood and adolescent cancer mortality. *Cancer* **120**, 2497–2506 (2014).
- Pui, C.H. *et al.* Childhood acute lymphoblastic leukemia: progress through collaboration. *J. Clin. Oncol.* **33**, 2938–2948 (2015).
- Rytting, M.E. *et al.* Augmented Berlin–Frankfurt–Münster therapy in adolescents and young adults (AYAs) with acute lymphoblastic leukemia (ALL). *Cancer* **120**, 3660–3668 (2014).
- Ram, R. *et al.* Adolescents and young adults with acute lymphoblastic leukemia have a better outcome when treated with pediatric-inspired regimens: systematic review and meta-analysis. *Am. J. Hematol.* **87**, 472–478 (2012).
- Faderl, S. *et al.* Adult acute lymphoblastic leukemia: concepts and strategies. *Cancer* **116**, 1165–1176 (2010).

- Kero, A.E. *et al.* Health conditions associated with metabolic syndrome after cancer at a young age: a nationwide register-based study. *Cancer Epidemiol.* **41**, 42–49 (2016).
- Essig, S. *et al.* Risk of late effects of treatment in children newly diagnosed with standard-risk acute lymphoblastic leukaemia: a report from the Childhood Cancer Survivor Study cohort. *Lancet Oncol.* **15**, 841–851 (2014).
- Topp, M.S. *et al.* Phase II trial of the anti-CD19 bispecific T cell-engager blinatumomab shows hematologic and molecular remissions in patients with relapsed or refractory B-precursor acute lymphoblastic leukemia. *J. Clin. Oncol.* **32**, 4134–4140 (2014).
- Topp, M.S. *et al.* Safety and activity of blinatumomab for adult patients with relapsed or refractory B-precursor acute lymphoblastic leukemia: a multicentre, single-arm, phase 2 study. *Lancet Oncol.* **16**, 57–66 (2015).
- Topp, M.S. *et al.* Targeted therapy with the T-cell-engaging antibody blinatumomab of chemotherapy-refractory minimal residual disease in B-lineage acute lymphoblastic leukemia patients results in high response rate and prolonged leukemia-free survival. *J. Clin. Oncol.* **29**, 2493–2498 (2011).
- Davila, M.L. *et al.* Efficacy and toxicity management of 19-28z CAR T cell therapy in B cell acute lymphoblastic leukemia. *Sci. Transl. Med.* **6**, 224ra25 (2014).
- Lee, D.W. *et al.* T cells expressing CD19 chimeric antigen receptors for acute lymphoblastic leukaemia in children and young adults: a phase 1 dose-escalation trial. *Lancet* **385**, 517–528 (2015).
- Maude, S.L. *et al.* Chimeric antigen receptor T cells for sustained remissions in leukemia. *N. Engl. J. Med.* **371**, 1507–1517 (2014).
- Raponi, S. *et al.* Flow cytometric study of potential target antigens (CD19, CD20, CD22, CD33) for antibody-based immunotherapy in acute lymphoblastic leukemia: analysis of 552 cases. *Leuk. Lymphoma* **52**, 1098–1107 (2011).
- Lucio, P. *et al.* BIOMED-I concerted action report: flow cytometric immunophenotyping of precursor B-ALL with standardized triple-stainings. BIOMED-1 concerted action investigation of minimal residual disease in acute leukemia: international standardization and clinical evaluation. *Leukemia* **15**, 1185–1192 (2001).
- Sotillo, E. *et al.* Convergence of acquired mutations and alternative splicing of CD19 enables resistance to CART-19 immunotherapy. *Cancer Discov.* **5**, 1282–1295 (2015).
- Grupp, S.A. *et al.* Durable remissions in children with relapsed/refractory ALL Treated with T cells engineered with a CD19-targeted chimeric antigen receptor (CTL019). *Blood* **126**, abstr. 681 (2015).
- Gardner, R. *et al.* Acquisition of a CD19-negative myeloid phenotype allows immune escape of MLL-rearranged B-ALL from CD19 CAR-T-cell therapy. *Blood* **127**, 2406–2410 (2016).
- Haso, W. *et al.* Anti-CD22-chimeric antigen receptors targeting B-cell precursor acute lymphoblastic leukemia. *Blood* **121**, 1165–1174 (2013).
- Shah, N.N. *et al.* Characterization of CD22 expression in acute lymphoblastic leukemia. *Pediatr. Blood Cancer* **62**, 964–969 (2015).
- Nguyen, K. *et al.* Factors influencing survival after relapse from acute lymphoblastic leukemia: a Children's Oncology Group study. *Leukemia* **22**, 2142–2150 (2008).
- Wayne, A.S. *et al.* Anti-CD22 immunotoxin RFB4(dsFv)-PE38 (BL22) for CD22-positive hematologic malignancies of childhood: preclinical studies and phase I clinical trial. *Clin. Cancer Res.* **16**, 1894–1903 (2010).
- Kreitman, R.J. *et al.* Phase I trial of anti-CD22 recombinant immunotoxin moxetumomab pasudotox (CAT-8015 or HA22) in patients with hairy cell leukemia. *J. Clin. Oncol.* **30**, 1822–1828 (2012).
- Kantarjian, H. *et al.* Results of inotuzumab ozogamicin, a CD22 monoclonal antibody, in refractory and relapsed acute lymphocytic leukemia. *Cancer* **119**, 2728–2736 (2013).
- Chevallier, P. *et al.* 90Y-labelled anti-CD22 epratuzumab tetraxetan in adults with refractory or relapsed CD22-positive B-cell acute lymphoblastic leukaemia: a phase 1 dose-escalation study. *Lancet Haematol.* **2**, e108–e117 (2015).
- Chevallier, P. *et al.* Vincristine, dexamethasone and epratuzumab for older relapsed/refractory CD22+ B-acute lymphoblastic leukemia patients: a phase II study. *Haematologica* **100**, e128–e131 (2015).
- Raetz, E.A. *et al.* Re-induction chemioimmunotherapy with epratuzumab in relapsed acute lymphoblastic leukemia (ALL): phase II results from Children's Oncology Group (COG) study ADVL04P2. *Pediatr. Blood Cancer* **62**, 1171–1175 (2015).
- Grant, B.W. *et al.* A phase 2 trial of extended induction epratuzumab and rituximab for previously untreated follicular lymphoma: CALGB 50701. *Cancer* **119**, 3797–3804 (2013).
- Kantarjian, H.M. *et al.* Inotuzumab ozogamicin versus standard therapy for acute lymphoblastic leukemia. *N. Engl. J. Med.* **375**, 740–753 (2016).
- Xiao, X., Ho, M., Zhu, Z., Pastan, I. & Dimitrov, D.S. Identification and characterization of fully human anti-CD22 monoclonal antibodies. *MAbs* **1**, 297–303 (2009).
- Kawalekar, O.U. *et al.* Distinct signaling of coreceptors regulates specific metabolism pathways and impacts memory development in CAR T cells. *Immunity* **44**, 712 (2016).
- Chevallier, P. *et al.* Simultaneous study of five candidate target antigens (CD20, CD22, CD33, CD52, HER2) for antibody-based immunotherapy in B-ALL: a monocentric study of 44 cases. *Leukemia* **23**, 806–807 (2009).
- Olejniczak, S.H., Stewart, C.C., Donohue, K. & Czuczman, M.S. A quantitative exploration of surface antigen expression in common B-cell malignancies using flow cytometry. *Immunol. Invest.* **35**, 93–114 (2006).



34. Kantarjian, H. *et al.* Inotuzumab ozogamicin, an anti-CD22–calicheamicin conjugate, for refractory and relapsed acute lymphocytic leukaemia: a phase 2 study. *Lancet Oncol.* **13**, 403–411 (2012).
35. Long, A.H. *et al.* 4-1BB costimulation ameliorates T cell exhaustion induced by tonic signaling of chimeric antigen receptors. *Nat. Med.* **21**, 581–590 (2015).
36. Till, B.G. *et al.* CD20-specific adoptive immunotherapy for lymphoma using a chimeric antigen receptor with both CD28 and 4-1BB domains: pilot clinical trial results. *Blood* **119**, 3940–3950 (2012).
37. Ramos, C.A. *et al.* Clinical responses with T lymphocytes targeting malignancy-associated  $\kappa$  light chains. *J. Clin. Invest.* **126**, 2588–2596 (2016).
38. Guo, B. *et al.* CD138-directed adoptive immunotherapy of chimeric antigen receptor (CAR)-modified T cells for multiple myeloma. *J. Cell. Immunother.* **2**, 28–35 (2016).
39. Ali, S.A. *et al.* T cells expressing an anti-B-cell maturation antigen chimeric antigen receptor cause remissions of multiple myeloma. *Blood* **128**, 1688–1700 (2016).
40. Ritchie, D.S. *et al.* Persistence and efficacy of second generation CAR T cell against the LeY antigen in acute myeloid leukemia. *Mol. Ther.* **21**, 2122–2129 (2013).
41. Borowitz, M.J. *et al.* Clinical significance of minimal residual disease in childhood acute lymphoblastic leukemia and its relationship to other prognostic factors: a Children's Oncology Group study. *Blood* **111**, 5477–5485 (2008).
42. Borowitz, M.J. *et al.* Prognostic significance of minimal residual disease in high risk B-ALL: a report from Children's Oncology Group study AALL0232. *Blood* **126**, 964–971 (2015).
43. Pui, C.H. *et al.* Clinical utility of sequential minimal residual disease measurements in the context of risk-based therapy in childhood acute lymphoblastic leukaemia: a prospective study. *Lancet Oncol.* **16**, 465–474 (2015).
44. Grupp, S.A. *et al.* Chimeric antigen receptor-modified T cells for acute lymphoid leukemia. *N. Engl. J. Med.* **368**, 1509–1518 (2013).
45. Jacoby, E. *et al.* CD19 CAR immune pressure induces B-precursor acute lymphoblastic leukaemia lineage switch exposing inherent leukaemic plasticity. *Nat. Commun.* **7**, 12320 (2016).
46. Walker, A.J. *et al.* Tumor antigen and receptor densities regulate efficacy of a chimeric antigen receptor targeting anaplastic lymphoma kinase. *Mol. Ther.* **25**, 2189–2201 (2017).
47. Watanabe, K. *et al.* Target antigen density governs the efficacy of anti-CD20-CD28-CD3  $\zeta$  chimeric antigen receptor-modified effector CD8<sup>+</sup> T cells. *J. Immunol.* **194**, 911–920 (2015).
48. Caruso, H.G. *et al.* Tuning sensitivity of CAR to EGFR density limits recognition of normal tissue while maintaining potent antitumor activity. *Cancer Res.* **75**, 3505–3518 (2015).
49. Turatti, F. *et al.* Redirected activity of human antitumor chimeric immune receptors is governed by antigen and receptor expression levels and affinity of interaction. *J. Immunother.* **30**, 684–693 (2007).
50. Qin, H., Haso, W., Nguyen, S.M. & Fry, T.J. Preclinical development of bispecific chimeric antigen receptor targeting both CD19 and CD22. *Blood* **126**, abstr. 4427 (2015).

## ONLINE METHODS

**Trial design and toxicity monitoring.** This phase 1, first-in-human, dose-escalation trial conducted at the Pediatric Oncology Branch of the National Cancer Institute (NCI) was designed to test the safety and feasibility of CD22-CAR T cell therapy in children and young adults, aged 1–30 years, with relapsed or refractory CD22-expressing hematopoietic malignancies that had not responded to or had recurred following standard treatment regimens. The protocol was approved by the NCI Institutional Review Board and the NIH Recombinant DNA Advisory Committee (NCT02315612). Written informed consent for participation was obtained from patients or their parents according to the Declaration of Helsinki. This report represents an interim analysis from the first 21 consecutively treated patients with pre-B-ALL who received CD22-CAR T cell infusions between December 2014 and August 2016, with a data cutoff of 1 June 2017. A total of 23 patients were enrolled, but in one case T lymphocyte numbers were inadequate for CAR cell production, and thus this patient was not treated in the study; in a second case, the diagnosis was diffuse large B cell lymphoma, which is not included in this analysis of efficacy in B-ALL.

A standard 3 + 3 phase 1 dose-escalation design was used. If two of six patients experienced DLT at dose level 1, safety would have been evaluated in a de-escalated dose of  $1 \times 10^5$  transduced T cells per kg body weight. Once the maximum tolerated dose (or the highest level evaluated) was reached, enrollment into an expansion cohort of a total of 12 patients in two strata proceeded in order to provide additional information regarding the feasibility, safety and efficacy of this treatment. In the expansion cohort, patients who previously received CD19-CAR T cells were evaluated as a separate stratum from CAR-naïve patients. All doses allowed a range of  $\pm 20\%$  of the prescribed dose to allow for potential variations in the cell products.

Dose-limiting toxicity was defined as any toxicity that was grade 3 or above considered possibly, probably or likely related to either the lymphodepletion regimen or the CD22-CAR T cells with the exception of low electrolyte levels responding to supplementation, tumor lysis syndrome, hypoalbuminemia, liver dysfunction resolved to below grade 2 within 14 d of onset, transient ( $< 72$ -h) grade 4 hepatic enzyme abnormality, pre-existing coagulopathy, grade 3 or 4 fever lasting 7 d or less, grade 3 diarrhea that resolved to grade 2 within 4 d, grade 3 nausea and/or anorexia, any infusion-related toxicity occurring within 24 h that would resolve with minimal intervention and grade 3 CRS. CRS was graded and managed on the basis of Lee *et al.*<sup>51</sup>. Additionally, subjects with abnormal blood counts at baseline due to bone marrow involvement were not evaluable for hematologic toxicity analysis.

To evaluate possible neurotoxic effects, psychologists administered a brief ( $< 1$ -h) neurocognitive battery to patients before (baseline) and at 1 month after (days 21–28) CD22-CAR T cell infusion. The test battery consisted of the NIH Toolbox computerized test<sup>1</sup> evaluating attention, working memory, cognitive flexibility and a paper-and-pencil test assessing processing speed<sup>2</sup>. At baseline and then at approximately 14 and 21 d post-infusion, the caregiver of the patient or the adult patient completed a neuro-symptom checklist that assessed fever, auditory or visual hallucinations, responsiveness to commands, disorientation, depressed mood and pain<sup>52</sup>.

**Eligibility.** Patients were eligible if their disease had recurred after standard upfront therapy and at least one salvage therapy. There was no limit on the number of previous salvage therapies the patient might have received. Prior allogeneic stem cell transplant was allowed if at least 100 d had elapsed since transplant, there was no evidence of graft-versus-host disease (GVHD) and the patient was off systemic immunosuppression for at least 30 d before enrollment. Patients who had received prior CD19-CAR therapy were eligible if at least 30 d had elapsed since CD19-CAR infusion and circulating levels of genetically modified cells were  $< 5\%$  as determined by flow cytometry.

Eligibility required a performance status of  $\geq 50\%$  by Karnofsky for patients  $> 16$  years of age or  $\geq 50\%$  using the Lansky scale for patients  $< 16$  years of age. Minimal weight for eligibility was 15 kg. Patients with asymptomatic CNS1 or CNS2 leukemia were eligible, whereas patients with symptomatic or CNS3 leukemia were ineligible, as previously described<sup>12</sup>. Patients with isolated CNS or testicular leukemia were not eligible.

Patients with uncontrolled intercurrent infection, other malignancies, illnesses or conditions that would limit their ability to tolerate or comply with the

study requirements were ineligible. Patients were also ineligible if they demonstrated seropositivity for HIV or hepatitis C virus (HCV) or positive testing for hepatitis B virus (HBV) surface antigen or if they had a history of hypersensitivity to the agents required for the treatment regimen. Other exclusion criteria included inadequate liver function, defined as total bilirubin  $> 2 \times$  the upper limit of normal (ULN) (except for patients with documented Gilbert's) or transaminase levels  $> 3 \times$  ULN, renal function  $< 60$  ml/min per  $1.73 \text{ m}^2$  or hyperleukocytosis ( $\geq 50,000$  circulating blasts/ $\mu\text{l}$  blood).

Systemic chemotherapy must have been completed  $> 2$  weeks before enrollment ( $> 6$  weeks for clofarabine or nitrosureas), radiation therapy must have been completed  $> 3$  weeks before enrollment, monoclonal antibody therapy must have been completed at least 30 d or 5 half-lives before enrollment, and investigational antineoplastic therapy must have been completed at least 30 d before enrollment. No washout period was required for intrathecal chemotherapy, hydroxyurea (provided no increase in dose in the 2 weeks before enrollment), standard maintenance ALL therapy or physiologic steroid replacement.

**CD22-CAR construct and manufacturing of CD22-CAR T cells.** The CD22-CAR contains a fully human single-chain fragment variable region generated from a human B cell phage library<sup>30</sup>, a CD8 transmembrane domain and CD3 zeta plus 4-1BB signaling chains (CD22.BB.z) as previously described and as illustrated in **Figure 1a**<sup>19,35</sup>. All patients received an identical preparative regimen consisting of fludarabine at a dose of  $25 \text{ mg/m}^2$  per day on days  $-4$ ,  $-3$  and  $-2$  and cyclophosphamide at a dose of  $900 \text{ mg/m}^2$  on day  $-2$ , with CD22-CAR T cell infusion on day 0.

CD22-CAR T cells were produced in the Cell Processing Section of the Department of Transfusion Medicine, NIH Clinical Center. This laboratory operates under principles of Good Manufacturing Practices and Good Clinical Laboratory Practice with established Standard Operating Procedures (SOPs) and/or protocols for sample receipt, processing, freezing and analysis. All patients underwent leukapheresis within 5 d of enrollment. Leukapheresed peripheral blood mononuclear cells were either placed directly into culture or cryopreserved before culture initiation on a subsequent day. In cases in which substantial numbers of myeloid cells were present in the apheresis products, elutriation and/or plastic adherence<sup>53</sup> was performed on the basis of evidence that such cells inhibited expansion<sup>54</sup>. The lentiviral vector containing CD22.BB.Z-CAR was produced by Lentigen. Cells were expanded in sterile bags in a  $37^\circ\text{C}$  incubator for 9 d, with an additional 3 d of culture permitted to allow resolution of intercurrent clinical events. If more than 3 d was required, cells were cryopreserved and then thawed immediately before infusion. Final product release criteria required the following: cell viability  $\geq 70\%$ , cell number within 20% of planned dose, % CAR T cells  $\geq 15\%$  as measured using CD22-Fc fusion protein, endotoxin 5 EU/ml, mycoplasma negativity, gram stain and culture negativity and vesicular stomatitis virus (VSV-G) DNA (as a surrogate marker for replication-competent lentivirus (RCL) negativity as determined by qPCR). In process, culture-based testing was also performed on an aliquot of the product at the National Gene Vector Laboratory (Indiana University) using assays for p24 antigen and product-enhanced reverse transcriptase assay (PERT) to complete testing for RCL.

**Response monitoring.** Baseline bone marrow aspirate and biopsy and lumbar puncture were performed within the 14 d before the start of the lymphodepletion preparative regimen, and then response was monitored via bone marrow aspirate and biopsy and lumbar puncture performed  $28 \pm 4$  d from cell infusion and at 2, 3, 6, 9 and 12 months. CR was defined by morphologic assessment of the bone marrow as M1 ( $< 5\%$  leukemic blasts) with no evidence of extramedullary disease. MRD was assessed through multiparametric flow cytometry conducted at the NCI Laboratory of Pathology using standard techniques.

**Cytokine assays, PCR and flow cytometry.** Plasma was cryopreserved before measurement of cytokines in a multiplex format according to manufacturer's instructions (Meso Scale Discovery, Gaithersburg, MD, USA). CD22-CAR T cell expansion was measured through qPCR (Life Technologies, Grand Island, NY, USA), which was adapted from published methods<sup>55</sup>. Briefly, measured CAR copies per 100 ng DNA were normalized to the input quantity of amplifiable DNA by measurement of the single-copy gene *CDKN1A*.

Specimens for flow cytometry were processed within 12 h of collection and stained with a panel of antibodies to quantify leukemic burden and measure CAR T cell numbers. Briefly, whole-blood lysis was performed using ammonium chloride before staining for 30 min at room temperature with the following two cocktails (antibody concentration according to manufacturer's recommendations): Cocktail A—CD16F1TC (clone DJ130c, Dako), CD19PE (clone SJ25C1, BD Biosciences), CD3PerCP (clone SK7, BD Biosciences), CD13PECy7 (L138, BD Biosciences), CD34APC (clone 8G12, BD Biosciences), CD14 APC H7 (MP9, BD Biosciences), CD56v450 (clone B159, BD Biosciences), CD45 v500 (clone HI30, BD Biosciences); and Cocktail B—CD66bF1TC (clone G10F5, BD Biosciences), CD22PE (clone S-HCL-1, BD Biosciences), CD34PerCP5.5 (clone 8G12, BD Biosciences), CD19PECy7 (clone SJ25C1, BD Biosciences), CD24APC (clone SN3 A5-2H10, eBioscience), CD45 APC H7 (clone 2D1, BD Biosciences), CD10BV421 (clone HI10a, BD Biosciences) and CD38BV510 (clone HB-7, BioLegend). At least 1 million cells were acquired per tube using an 8-color multiparametric approach on a 3-laser FACS Canto II (BD Biosciences, San Jose, CA) with DiVa 6.1.1 software and were analyzed by FCS Express 4 software (DeNovo Software, Los Angeles, CA). The validated limit of detection of leukemic blasts with this assay was 0.002% of cells.

CD22-CAR T cells were measured using a CD22-Fc (R&D Systems, Minneapolis, MN). CAR T cells were detected using the following cocktail: CD20F1TC (B-Ly1, Dako), CD10PE (clone HI10a, BD), CD34PerCP5.5 (clone 8G12, BD Biosciences), CD19PECy7 (clone SJ25C1, BD Biosciences), CD22-Fc-APC (R&D Systems), CD3APC-H7 (clone SK7, BD Biosciences), CD14 v450 (Mtems), CD3APC-H7 (clone SK7, BD Biosciences), CD19PECy7 (clone SJ25C1, BD Biosciences) and CD10PE (clone W8E7, BD Biosciences, San Jose, CA, USA). Circulating CAR T cell numbers were calculated on the basis of estimated blood volume and measured absolute lymphocyte counts.

**CD19 and CD22 flow cytometric site density determination.** CD22 and CD19 site density on blasts was enumerated through flow cytometry according to manufacturer's instructions (QuantiBRITE Beads, BD Biosciences, San Jose, CA, USA). The antibody bound per cell (ABC) was determined as previously described<sup>56,57</sup> for anti-CD19PE (clone SJ25C1) and anti-CD22PE (clone S-HCL-1) (BD Biosciences, San Jose, CA) on leukemic blasts using saturating concentrations of antibody and the BD Biosciences QuantiBRITE system (QuantiBRITE standard beads and QuantiCALC software) for fluorescence quantification. The ABC value represents the mean value of the maximum capacity of each cell to bind the antibody. QuantiBRITE PE beads are precalibrated standard beads containing known numbers of PE molecules bound per bead. QuantiBRITE beads were acquired on a FACSCanto II (BD Biosciences, San Jose, CA) on the same day at the same instrument settings as the individual patient specimens. A standard curve comparing the geometric mean of fluorescence to known PE content of the QuantiBRITE beads was constructed using QuantiCALC software. The regression analysis, slope, intercept and correlation coefficient were determined. By gating based upon immunophenotype, blasts were distinguished from normal cells and the geometric mean fluorescence of CD19 and CD22 staining was reported for each population. The ABC values were generated from the measured geometric mean fluorescence of the gated cells using the QuantiBRITE standard curve. ABC values were only determined for populations containing 100 or greater events to achieve adequate precision. The geometric mean fluorescence of T cells and NK cells stained with the B cell antibodies (negative control) has been previously determined, and the negative ABC range was used to confirm positivity versus negativity. In addition, blasts with anti-CD19 or anti-CD22 staining less than or equal to that of T cells (internal negative control) were considered negative.

**CRISPR-Cas9 editing of cell lines.** Guide RNAs were designed from the GeCKO human single guide RNA (sgRNA) library, cloned into LentiCRISPR v2 plasmid (Addgene Plasmid 52961) and transformed into *Stbl3 Escherichia coli* (hCD19 F: 5'-CACCGTGAATGTTTCGGACCTAGG-3', hCD19 R: 5'-AAACCTAGG TCCGAAACATTCCAC-3', hCD22 F: 5'-CACCGTCTCCTTCTCGAATCGGC AT-3' and hCD22 R: 5'-AAACATGCCGATTTCGAGAAGGAGAC-3'). Plasmids were cotransfected with packaging plasmids RRE, pMD-G and REV into LentiX HEK293T cells (Clontech, Mountain View, CA, USA). After 2 d, CRISPR supernatants were harvested and filtered through a 0.45- $\mu$ m low-protein-binding

membrane (Millipore, Billerica, Massachusetts, USA), concentrated using Lenti-X concentrator (Clontech, Mountain View, CA, USA), resuspended in PBS and used immediately or stored at  $-80^{\circ}\text{C}$ . For viral transduction,  $1 \times 10^5$  leukemia cells were incubated with 10  $\mu$ l of concentrated viral supernatant for 2 d, followed by expansion in RPMI with 10% FBS, penicillin/streptomycin and GlutaMAX. Cell phenotype was assessed through flow cytometry, which was followed by sorting of cells with phenotypic alterations and single-cell cloning. Sequencing was performed on single-cell clones to confirm genotypic alterations by Platinum PCR Supermix High Fidelity Kit (Invitrogen) (hCD19 F: 5'-TCTCCCTCTCTGGGTG-3', hCD19 R: 5'-CTCTCCCTCCAGATCTCAG-3', hCD22 F: 5'-AGGAGGGAAGGGGTACTG-3' and hCD22 R: 5'-AGCCAACG TTTTGGATCTTCAG-3'). To obtain cell lines with various CD22 site densities, a plasmid with the complete cDNA sequence for human CD22 (Origene) was retransduced into the CD22<sup>-</sup> cell line at different concentrations. Cell lines were cloned from single cells with resultant cell lines including CD22<sup>-</sup>, CD19<sup>-</sup>, CD22<sup>lo</sup> and high-CD22-site-density (CD22<sup>hi</sup>) cell lines. QuantiBRITE Beads (BD Biosciences, San Jose, CA, USA) were used, as per the above description, to identify site density of CRISPR-Cas9-modified cell lines.

**CD19-CD22-bispecific CAR.** A bispecific CAR construct was developed using a CD19-binding domain derived from a clinically active CD19-CAR<sup>12</sup> and a CD22-binding domain used for the CD22-CAR reported herein. A schematic of the CD19-CD22-bispecific CAR is shown in **Figure 4a** and the full sequence is provided **Supplementary Figure 6**.

The bispecific CAR was transduced onto human T cells using lentiviral vectors. The potency of the bispecific CAR was tested against the CRISPR-Cas9 knockout cell lines as well as the parental Nalm6 ALL cell line. Cytokine production was analyzed in cell co-culture supernatants using R&D ELISA kits for IFN- $\gamma$  and IL-2, following the product protocol (R&D Systems, Minneapolis, MN, USA). In brief, CD22-CAR T cells were washed three times and co-incubated with varying tumor target cells in a 1:1 effector-to-target ratio for 16–20 h. Supernatant was collected from co-incubation and used for evaluation of cytokine production. Of note, supernatant was diluted 1:10 in medium for IFN- $\gamma$  analysis. Supernatant was not diluted for IL-2 evaluation. Optical density was determined within 30 min using a microplate reader set to 450 nm with a wavelength correction of 540 nm. *In vitro* killing was analyzed using an IncuCyte assay (Essen BioScience). CAR cells were co-incubated with GFP<sup>+</sup> tumor target cells at a range of effector-to-target ratios. At the 24-h time point, green fluorescent units per well (GFU/well) was calculated using IncuCyte software, standardized to baseline GFU/well and normalized to tumor-only wells. Assays were performed in triplicate, and data are representative of multiple repeat experiments.

**Xenograft models.** *In vivo* analysis of CAR activity was conducted using a xenograft model with NOD.Cg-*Prkdc<sup>scid</sup>Il2rg<sup>tm1Wjl</sup>/SzJ* (NSG, Jackson Laboratories) mice. Mice were injected intravenously with  $1 \times 10^6$  GFP<sup>+</sup> NALM6 tumor cells on day 0. On day 3, CAR-transduced T cells or mock-transduced T cells were injected as indicated. Mice received luciferin-D intraperitoneal injections and were imaged using *in vivo* imaging system (IVIS) technology. All mouse studies were approved by the NCI Animal Care and Use Committee.

**Genomic profiling.** All primary patient samples were collected on institutional review board (IRB)-approved protocols for biological specimen research. Leukemia samples from bone marrow specimens containing greater than 90% leukemia were isolated by density gradient separation using Lymphocyte Separation Medium (Lonzo). The cells were lysed and nucleic acid extraction was performed using Qiagen AllPrep Kits (Qiagen) per the manufacturer's protocol. DNA and RNA were quantified and assessed for quality using an Agilent 2100 BioAnalyzer. Polyadenylated RNA libraries were generated and sequenced using TruSeq 4.0 chemistry on a HiSeq2500 (Illumina). Whole-exome data were generated using Agilent SureSelectXT Human All Exon V5 and TruSeq V4 chemistry and sequenced to a median of 300 $\times$  coverage on a HiSeq2500 (Illumina).

Whole-exome and RNA-seq data were analyzed and mapped using the CCR Collaborative Bioinformatics Resource (CCBR) pipeline (<https://bioinformatics.cancer.gov/>). Reads were aligned to reference genome Hg19. Somatic variant calling was performed using MuTect<sup>58</sup> and copy number alterations were



analyzed using Nexus Copy Number Discovery Edition no. 9. (BioDiscovery). The integrity of the *CD22* gene was interrogated by manual inspection using Integrative Genome Viewer (IGV). RNA-seq reads for each sample were trimmed of their adaptors and low-quality bases using Trimmomatic software and aligned with reference human Hg38 and Gencode V24 transcripts using STAR software. Expression of *CD22* transcript was evaluated using log<sub>2</sub> RPKM values from the RNA-seq data.

**Statistical analyses.** Doses of CD22-CAR-transduced T cells were administered in a standard 3 + 3 dose-escalation design until MTD was determined. After treatment of the first patient in the first cohort, there was a 4-week (28-d) safety assessment before treatment of the second patient. Subsequent patients in a cohort were treated after a 1-week safety assessment period following cell infusion. Patients were enrolled sequentially; therefore, enrollment did not proceed to a higher dose level until all patients had been treated in the prior cohort and the last patient treated on the completed cohort had been observed for at least 4 weeks. If a minimum of  $1 \times 10^5$  CD22-CAR-transduced T cells per kg body weight could not be obtained for infusion, the patient was treated but was not evaluated for toxicity or response and the treatment was considered a feasibility failure. Up to six evaluable patients were enrolled in cohorts 1–4 (24 patients total in order to determine MTD; in addition, the study allowed up to 3 patients to be replaced in each of dose cohorts 1–3 (9 additional patients) owing to inability to achieve target doses). In addition, the study allowed for six total unevaluable patients (patients enrolled, but who could not receive cells either owing to physical deterioration or withdrawn consent during cell growth).

**Life Sciences Reporting Summary.** Further information on experimental design and reagents is available in the Life Sciences Reporting Summary.

**Data availability.** Patient-related data that were not included in the manuscript may be restricted, as they were generated in the context of an ongoing clinical trial and may be subject to patient confidentiality. All other data that support the findings of this study are available from the corresponding author upon reasonable request.

51. Lee, D.W. *et al.* Current concepts in the diagnosis and management of cytokine release syndrome. *Blood* **124**, 188–195 (2014).
52. Weintraub, S. *et al.* Cognition assessment using the NIH Toolbox. *Neurology* **80** (Suppl. 3), S54–S64 (2013).
53. Stroncek, D.F. *et al.* Elutriated lymphocytes for manufacturing chimeric antigen receptor T cells. *J. Transl. Med.* **15**, 59 (2017).
54. Stroncek, D.F. *et al.* Myeloid cells in peripheral blood mononuclear cell concentrates inhibit the expansion of chimeric antigen receptor T cells. *Cytotherapy* **18**, 893–901 (2016).
55. Kalos, M. *et al.* T cells with chimeric antigen receptors have potent antitumor effects and can establish memory in patients with advanced leukemia. *Sci. Transl. Med.* **3**, 95ra73 (2011).
56. Tembhare, P.R. *et al.* Quantification of expression of antigens targeted by antibody-based therapy in chronic lymphocytic leukemia. *Am. J. Clin. Pathol.* **140**, 813–818 (2013).
57. Jasper, G.A. *et al.* Variables affecting the quantitation of CD22 in neoplastic B cells. *Cytometry B Clin. Cytom.* **80**, 83–90 (2011).
58. Cibulskis, K. *et al.* Sensitive detection of somatic point mutations in impure and heterogeneous cancer samples. *Nat. Biotechnol.* **31**, 213–219 (2013).

## Life Sciences Reporting Summary

Nature Research wishes to improve the reproducibility of the work that we publish. This form is intended for publication with all accepted life science papers and provides structure for consistency and transparency in reporting. Every life science submission will use this form; some list items might not apply to an individual manuscript, but all fields must be completed for clarity.

For further information on the points included in this form, see [Reporting Life Sciences Research](#). For further information on Nature Research policies, including our [data availability policy](#), see [Authors & Referees](#) and the [Editorial Policy Checklist](#).

### ► Experimental design

#### 1. Sample size

Describe how sample size was determined.

As stated in the methods, all sequentially enrolled patients with ALL were included in the analysis through a specific cutoff date to ensure adequate follow up

#### 2. Data exclusions

Describe any data exclusions.

No data was excluded from the analysis

#### 3. Replication

Describe whether the experimental findings were reliably reproduced.

All attempts at replication of the pre-clinical experiments were successful

#### 4. Randomization

Describe how samples/organisms/participants were allocated into experimental groups.

In the murine experiments, mice were injected with leukemia and randomly distributed (without bias from the luciferase imaging of leukemia burden) to treatment groups

#### 5. Blinding

Describe whether the investigators were blinded to group allocation during data collection and/or analysis.

Mouse imaging was performed by an operator who was blinded to treatment group.

Note: all studies involving animals and/or human research participants must disclose whether blinding and randomization were used.

#### 6. Statistical parameters

For all figures and tables that use statistical methods, confirm that the following items are present in relevant figure legends (or in the Methods section if additional space is needed).

n/a Confirmed

- ☐ ☒ The exact sample size ( $n$ ) for each experimental group/condition, given as a discrete number and unit of measurement (animals, litters, cultures, etc.)
- ☐ ☒ A description of how samples were collected, noting whether measurements were taken from distinct samples or whether the same sample was measured repeatedly
- ☐ ☒ A statement indicating how many times each experiment was replicated
- ☐ ☒ The statistical test(s) used and whether they are one- or two-sided (note: only common tests should be described solely by name; more complex techniques should be described in the Methods section)
- ☒ ☐ A description of any assumptions or corrections, such as an adjustment for multiple comparisons
- ☐ ☒ The test results (e.g.  $P$  values) given as exact values whenever possible and with confidence intervals noted
- ☐ ☒ A clear description of statistics including central tendency (e.g. median, mean) and variation (e.g. standard deviation, interquartile range)
- ☐ ☒ Clearly defined error bars

See the web collection on [statistics for biologists](#) for further resources and guidance.

## ► Software

Policy information about [availability of computer code](#)

### 7. Software

Describe the software used to analyze the data in this study.

Statistics were performed using GraphPad Prism. Details of the sequencing analysis are included in the Methods.

For manuscripts utilizing custom algorithms or software that are central to the paper but not yet described in the published literature, software must be made available to editors and reviewers upon request. We strongly encourage code deposition in a community repository (e.g. GitHub). *Nature Methods* [guidance for providing algorithms and software for publication](#) provides further information on this topic.

## ► Materials and reagents

Policy information about [availability of materials](#)

### 8. Materials availability

Indicate whether there are restrictions on availability of unique materials or if these materials are only available for distribution by a for-profit company.

There are no restrictions on availability of material described.

### 9. Antibodies

Describe the antibodies used and how they were validated for use in the system under study (i.e. assay and species).

Antibodies used for flow cytometry are listed in Methods. Clinical samples were analyzed in CLIA laboratories at the NIH and were validated in this laboratory. Details on the site density measurement assay is included in Methods.

### 10. Eukaryotic cell lines

a. State the source of each eukaryotic cell line used.

The parental Nalm6 cell line was provided by ATCC

b. Describe the method of cell line authentication used.

The Nalm6 cell line formally authenticated by HLA typing and verified to express the relevant antigens (CD19 and CD22) prior to each experiment.

c. Report whether the cell lines were tested for mycoplasma contamination.

All cell lines were tested for mycoplasma contamination and confirmed to be negative

d. If any of the cell lines used are listed in the database of commonly misidentified cell lines maintained by [ICLAC](#), provide a scientific rationale for their use.

No commonly mis-identified cell lines were used

## ► Animals and human research participants

Policy information about [studies involving animals](#); when reporting animal research, follow the [ARRIVE guidelines](#)

### 11. Description of research animals

Provide details on animals and/or animal-derived materials used in the study.

Male and female Non-Obese Diabetic, SCID, gamma KO (NSG) mice were use for xenograft studies.

Policy information about [studies involving human research participants](#)

### 12. Description of human research participants

Describe the covariate-relevant population characteristics of the human research participants.

Required information is included in supplemental table.



# Flow Cytometry Reporting Summary

Form fields will expand as needed. Please do not leave fields blank.

## ▶ Data presentation

For all flow cytometry data, confirm that:

- ☒ 1. The axis labels state the marker and fluorochrome used (e.g. CD4-FITC).
- ☒ 2. The axis scales are clearly visible. Include numbers along axes only for bottom left plot of group (a 'group' is an analysis of identical markers).
- ☐ 3. All plots are contour plots with outliers or pseudocolor plots.
- ☒ 4. A numerical value for number of cells or percentage (with statistics) is provided.

## ▶ Methodological details

5. Describe the sample preparation.	Murine bone marrow (see Methods); human blood, bone marrow, cerebrospinal fluid. Processing of human samples per CLIA certified lab.
6. Identify the instrument used for data collection.	Becton Dickinson (BD) Fortessa for preclinical samples, BD Canto for Clinical samples.
7. Describe the software used to collect and analyze the flow cytometry data.	FlowJo used for analysis of preclinical samples, analysis of human samples per CLIA certified lab.
8. Describe the abundance of the relevant cell populations within post-sort fractions.	N/A
9. Describe the gating strategy used.	See supplemental data

Tick this box to confirm that a figure exemplifying the gating strategy is provided in the Supplementary Information. ☒